Monte Carlo simulated beam quality and perturbation correction factors for ionization chambers in monoenergetic proton beams

Kretschmer, Jana; Dulkys, Anna; Brodbek, Leonie; Stelljes, Tenzin Sonam; Looe, Hui Khee; Poppe, Bjoern

Published in:
Medical Physics

DOI:
10.1002/mp.14499

Monte Carlo simulated beam quality and perturbation correction factors for ionization chambers in monoenergetic proton beams

Jana Kretschmer[a)]
University Clinic for Medical Radiation Physics, Medical Campus Pius Hospital, Carl-von-Ossietzky University, Oldenburg, Germany

Anna Dulkys
University Clinic for Medical Radiation Physics, Medical Campus Pius Hospital, Carl-von-Ossietzky University, Oldenburg, Germany
Department of Radiation Therapy, Helios Clinics Schwerin, Schwerin, Germany

Leonie Brodbek
University Clinic for Medical Radiation Physics, Medical Campus Pius Hospital, Carl-von-Ossietzky University, Oldenburg, Germany
Department of Radiation Oncology, University Medical Center Groningen, University of Groningen, Groningen, The Netherlands

Tenzin Sonam Stelljes, Hui Khee Looe, and Björn Poppe
University Clinic for Medical Radiation Physics, Medical Campus Pius Hospital, Carl-von-Ossietzky University, Oldenburg, Germany

(Received 26 May 2020; revised 19 August 2020; accepted for publication 8 September 2020; published 14 October 2020)

Purpose: Beam quality correction factors provided in current codes of practice for proton beams are approximated using the water-to-air mass stopping power ratio and by assuming the proton beam quality related perturbation correction factors to be unity. The aim of this work is to use Monte Carlo simulations to calculate energy dependent beam quality and perturbation correction factors for a set of nine ionization chambers in proton beams.
Methods: The Monte Carlo code EGSnrc was used to determine the ratio of the absorbed dose to water and the absorbed dose to the sensitive air volume of ionization chambers f_{Q_0} related to the reference photon beam quality (^{60}Co). For proton beams, the quantity f_Q was simulated with GATE/Geant4 for five monoenergetic beam energies between 70 MeV and 250 MeV. The perturbation correction factors for the air cavity, chamber wall, chamber stem, central electrode, and displacement effect in proton radiation were investigated separately. Additionally, the correction factors of cylindrical chambers were investigated with and without consideration of the effective point of measurement.
Results: The perturbation factors p_Q were shown to deviate from unity for the investigated chambers, contradicting the assumptions made in dosimetry protocols. The beam quality correction factors for both plane-parallel and cylindrical chambers positioned with the effective point of measurement at the measurement depth were constant within 0.8%. An increase of the beam quality correction factors determined for cylindrical ionization chambers placed with their reference point at the measurement depth with decreasing energy is attributed to the displacement perturbation correction factors p_{dis}, which were up to 1.045 ± 0.1% for the lowest energy and 1.005 ± 0.1% for the highest energy investigated. Besides p_{dis}, the largest perturbation was found for the chamber wall where the smallest p_{wall} determined was 0.981 ± 0.3%.
Conclusions: Beam quality correction factors applied in dosimetry with cylindrical chambers in monoenergetic proton beams strongly depend on the positioning method used. We found perturbation correction factors different from unity. Consequently, the approximation of ionization chamber perturbations in proton beams by the respective water-to-air mass stopping power ratio shall be revised.
 [https://doi.org/10.1002/mp.14499]

Key words: correction factors, effective point of measurement, EGSnrc, GATE/Geant4, proton dosimetry

1. INTRODUCTION

Ionization chambers used in radiation therapy are generally calibrated under ^{60}Co radiation with beam quality Q_0. The measurement with such a calibrated chamber in a monoenergetic proton field having a different beam quality Q leads to a change in the chambers' dose response so that a correction with a beam quality correction factor k_{Q,Q_0} is required.[1] Note that this factor is referred to as k_Q whenever the reference beam quality is ^{60}Co radiation.[1] k_Q inherits the beam quality related changes in the mean energy needed to produce an ion pair in air W_{a}, the water-to-air mass stopping power ratio $s_{\mathrm{w,a}}$,

and the ionization chamber specific perturbation correction p.[1] k_Q depends on the chamber type and can be determined either experimentally[2–5] or using Monte Carlo simulations by calculating the ratio of the absorbed dose to water D_w and the absorbed dose to the sensitive air volume of the ionization chamber D_{Cham} at both beam qualities.[6–8] Depending on the respective beam quality, this ratio is referred to as f_Q or f_{Q_0} and can also be described by the product of $(s_{w,a})_{Q/Q_0}$ and p_{Q/Q_0}.[6–9]

Current dosimetry protocols, like the IAEA TRS-398[1] and the German DIN6801-1[10] assume that the perturbation correction factor p_Q can be approximated as unity for proton beams such that f_Q is described solely by $(s_{w,a})_Q$ and the ionization chamber specific perturbations are only considered by a relatively large uncertainty for f_Q of up to 1.3%.[1] The German code of practice DIN6801-1[10] states that the uncertainty in assuming p_Q being equal to unity is 0.1%. Together with the uncertainty for $(s_{w,a})_Q$, this leads to an uncertainty for f_Q of 1.5%. Moreover, DIN6801-1 suggests a constant f_Q and k_Q for monoenergetic proton beams with residual ranges larger than 1.5 cm by arguing that the variance in k_Q is 0.2%.[10]

The assumptions in the dosimetry protocols were questioned in the past. With the motivation to reduce the uncertainty of p_Q, f_Q and k_Q for ionization chamber measurements in monoenergetic proton beams, several Monte Carlo based studies were carried out in recent years.[6–9,11] Monte Carlo simulated f_Q and/or k_Q factors for monoenergetic proton beams were calculated by Gomà et al.,[6] Wulff et al.,[9] Gomà and Sterpin,[7] and Baumann et al.[8] for several ionization chambers under consideration of the latest ICRU Report 90.[12] In these studies, all factors were determined for various incident proton energies. Furthermore, the perturbation correction factors p_Q were individually investigated by Lourenço et al.[11] and Baumann et al.[8]

Gomà et al.[6] determined k_Q for a set of three cylindrical and nine plane-parallel ionization chambers with the Monte Carlo Code PENH[13] in combination with GAMOS,[14] which is based on Geant4.[15] Wulff et al.[9] investigated ionization chamber calculations in proton beams with the Monte Carlo Code TOPASv3.1.p1[16] based on GEANT4.10.3.p1[15] and determined f_Q factors for a Farmer type and a plane-parallel ionization chamber. Lourenço et al.[11] used the Monte Carlo Code FLUKA[17] and determined p_Q for three plane-parallel ionization chambers, which deviate from unity by up to 1%. Gomà and Sterpin[7] presented k_Q factors for 15 ionization chambers, which were also determined with the Monte Carlo code PENH.[13] More recently, Baumann et al.[8] presented k_Q factors for six plane-parallel and four cylindrical ionization chambers that were simulated with TOPASv3.1.p1[16]/Geant4.10.03.p01.[15] Comparing their f_Q to literature, Baumann et al. found differences to Gomà et al.[6] of up to 0.9%, differences to Wulff et al.[9] of 0.5% and differences to the study by Gomà and Sterpin[7] of up to 1.2%, which were predominantly found for high proton energies. In addition, Baumann et al. simulated perturbation correction factors for the individual chamber parts of one cylindrical ionization chamber and found an overall value of $p_Q = 0.987 \pm 0.7\%$, where the perturbation from the chamber wall had the largest contribution by 1.5%.[8] Compared to photon beam dosimetry, there is still a strong deficiency of chamber specific correction factors in the literature valid for proton beams.

In this work, the beam quality correction factors k_Q and perturbation correction factors p_Q were calculated for nine ionization chambers in monoenergetic proton beams with incident energies between 70 MeV and 250 MeV using Monte Carlo simulations. Three of the chambers investigated were cylindrical ionization chambers for which to our knowledge k_Q or p_Q factors have not been determined so far for proton fields. While the absorbed dose to water and the absorbed dose to the sensitive air volume in the ^{60}Co field were calculated with the EGSnrc code system (Version 2019a),[18,19] the proton radiation related quantities were determined in GATE V8.0[20]/Geant4 10.04.p01.[15] In contrast to the publications in the literature, f_Q and k_Q for cylindrical chambers were not only determined for the positioning with their reference points placed at the measurement depth, but also under consideration of the chambers' effective point of measurement (EPOM). In addition, the perturbation correction factors p_Q for the ionization chambers were analyzed with respect to the contributions from the individual chamber components comprising the perturbation by the air cavity, chamber wall, chamber stem, central electrode, and the displacement effect.

2. MATERIALS AND METHODS

2.A. Calculated quantities

The beam quality correction factor k_Q calculated for various ionization chambers is defined as follows:

$$k_Q = \frac{\left(\frac{D_w}{D_{Cham}}\right)_Q}{\left(\frac{D_w}{D_{Cham}}\right)_{Q_0}} \cdot \frac{(W_a)_Q}{(W_a)_{Q_0}} = \frac{f_Q}{f_{Q_0}} \cdot \frac{(W_a)_Q}{(W_a)_{Q_0}}$$

where $\left(\frac{D_w}{D_{Cham}}\right)_{Q/Q_0}$ is the ratio of the absorbed dose to water D_w and the absorbed dose to the chamber's sensitive air volume D_{Cham} at the proton beam quality Q or reference beam quality Q_0, and $(W_a)_{Q/Q_0}$ is the mean energy needed to produce an ion pair in air at the respective beam quality.[6] The ratio $\frac{(W_a)_Q}{(W_a)_{Q_0}}$ is provided in ICRU Report 90.[12] The ratios $\left(\frac{D_w}{D_{Cham}}\right)_Q$ and $\left(\frac{D_w}{D_{Cham}}\right)_{Q_0}$ are also referred to as the so-called f_Q and f_{Q_0} factors, respectively.[6–9] In this case the proton beam specific factor f_Q is defined by:

$$f_Q = (s_{w,a})_Q \cdot p_Q$$

where $(s_{w,a})_Q$ is the stopping power ratio of water and air at the measurement point in the beam quality Q and p_Q is the perturbation correction factor that accounts for the perturbation by the individual components of the ionization chamber causing the deviation from ideal Bragg-Gray detector conditions.[1,10] For cylindrical ionization chambers p_Q is given by:

TABLE I. Simulation settings in EGSnrc used to determine the f_{Q_0} factors for various ionization chambers.

Item name	Description	References
Code, version, release date	egs_chamber/EGSnrc (version 2019a), released on May 8, 2019	Kawrakow[18], Kawrakow et al.,[19] Wulff et al.[23]
Validation	Fano cavity test passed with 0.1% accuracy	Kawrakow[24]
Source description	10 × 10 cm^2 parallel beam with ^{60}Co spectrum	Mora et al.[25]
Cross sections and transport parameters		
Brems cross sections	BH	
Photon cross sections	xcom	
Radiative Compton corrections	Off	
Compton cross sections	Default	
Photonuclear cross sections	Default	
Pair cross sections	BH	
Spin effects	On	
Brems angular sampling	KM	
Electron Impact Ionization	Off	
Triplet production	Off	
Bound Compton scattering	norej	
Pair angular sampling	Simple	
Photoelectron angular sampling	On	
Rayleigh scattering	On	
Atomic relaxations	On	
Photonuclear attenuation	Off	
Boundary crossing algorithm	Exact	
Electron-step algorithm	EGSnrc	
Global Ecut	0.512 MeV	
Global Pcut	0.001 MeV	
Global Smax	1.00E + 10	
ESTEPE	0.25	
Ximax	0.5	
Skin depth for BCA	3	
Variance reduction techniques		
photon cross-section enhancement	XCSE enhancement factor = 512 within a region surrounding the scoring geometry of 1 cm	
Russian Roulette	Rejection factor = 512, Esave = 521 keV	
Scored quantities	Dose in sensitive volume	
# histories/statistical uncertainty	20 single batches on a cluster were used with 1E9 or 1E8 histories each	
Timing	The equivalent total simulation time for one point on a single CPU was up to 320 h	
Statistical methods	batch method	Seco and Verhaegen[45]
Postprocessing	Dose from the output file is extracted with MATLAB R2019b[46]	

$$p_Q = p_{cav} \cdot p_{dis} \cdot p_{cel} \cdot p_{wall} \cdot p_{stem}$$

where p_{cav} corrects for the perturbation from the extended air cavity, p_{dis} is the correction factor for the displacement effect, p_{cel} is central electrode correction, p_{wall} is the outer electrode or wall material correction, and p_{stem} is the chamber stem correction.[21] For plane-parallel ionization chambers the equation reduces to:[1,22]

$$p_Q = p_{wall} \cdot p_{cav}$$

The factors f_{Q_0}, f_Q, k_Q, and p_Q, were investigated individually for various cylindrical and plane-parallel ionization chambers.

2.B. Monte Carlo simulation of f_{Q_0}

The f_{Q_0}ctor was determined with Monte Carlo simulations in egs_chamber/EGSnrc (version 2019a).[18,19,23] This code has been shown to pass the fano cavity test with 0.1% accuracy[24] and is suitable for ionization chamber simulations in photon fields. To simulate the ratio f_{Q_0}, the definition of the calibration conditions in IAEA TRS-398[1] and DIN6801-1[10] is adopted. The absorbed dose to the ionization chamber $D_{Cham,Q_0}$was scored by placing the investigated chamber with its reference point at a depth z_{Q_0} of 5 cm in a 30 × 30 × 30 cm^3 water phantom irradiated with a 10 × 10 cm^2 field of ^{60}Co radiation. For the determination of

TABLE II. Comparison of the definition of reference conditions for monoenergetic proton beams between DIN6801-1[10] and IAEA TRS-398.[1]

	DIN6801-1	IAEA TRS-398
Phantom material	Water	Water
Field size	10×10 cm^2	10×10 cm^2
Depth z	$E > 100$ MeV: 3 cm $E < 100$ MeV: depending on energy	3 cm
Chamber type	$R_{res} \geq 1.5$ cm: compact chambers $R_{res} < 1.5$ cm: suitable, small plane-parallel chambers or suitable, small compact chambers	$R_{res} \geq 0.5$ g/cm^2: cylindrical and plane-parallel $R_{res} < 0.5$ g/cm^2: plane-parallel
Chamber positioning	Effective point of measurement	Reference point

D_{w,Q_0}, a cylinder with a radius of 1 cm and a thickness of 250 µm was used as scoring volume and positioned with its center at the measurement depth z_{Q_0}.[6–8] The source was defined as parallel beam using the ^{60}Co spectrum from Mora et al.[25] An overview on the simulation settings used in EGSnrc is provided in Table I according to the recommendations of Sechopoulos et al.[26]

2.C. Monte Carlo simulations of p_Q and f_Q

At the time of writing the definition of reference conditions for monoenergetic proton beams differs between the German code of practice DIN6801-1[10] and the international IAEA TRS-398[1] code of practice. An overview of the definitions is shown in Table II. While both protocols state that reference dosimetry should be performed in water and for a field size of 10×10 cm^2, the recommendations for the positioning of ionization chambers and the measurement depth differ. According to DIN6801-1, ionization chambers shall be positioned at a measurement depth of 3 cm for monoenergetic proton fields with $E \geq 100$ MeV while the measurement depth for lower proton energies is to be decided depending on the energy. For the positioning of cylindrical ionization chambers, DIN6801-1 states that the chamber specific EPOM should be considered. This is done by placing the reference point or central axis of the cylindrical chamber by a shift Δz_Q further down in the water phantom. This shift Δz_Q needs to be determined for each chamber individually and can be approximated by 0.75 times the radius of the sensitive air volume of the chamber.[10] IAEA TRS-398 only explicitly defines reference conditions for energy modulated beams and comments that in the case of monoenergetic proton beams, reference dosimetry shall be performed in the plateau region at 3 cm depth. It is suggested to only use plane-parallel chambers for residual ranges $R_{res} < 0.5$ g/cm^2 and to position ionization chambers with their reference points at the measurement depth.[1] It should be mentioned that the IAEA TRS-398 is currently being updated.[7]

In this work, f_Q and p_Q were determined at a depth z_Q of 2 cm in a $40 \times 40 \times 40$ cm^3 water phantom. The depth was chosen to slightly differ from the recommendations in the two mentioned codes of practice because this allows a comparison to f_Q and k_Q determined in the literature.[6–9,11] Simulations were performed for incident proton energies between 70 MeV ($R_{res} = 2.18$ cm) and 250 MeV ($R_{res} = 36.69$ cm). The influence of the positioning method of cylindrical ionization chambers was investigated by simulating the f_Q factors under consideration of the EPOM (reference point at depth $z_Q + \Delta z_Q$) as well as by placing the chambers with their reference points at the measurement depth z_Q.

The Monte Carlo simulations for f_Q and p_Q in proton beams were performed with the code GATE V8.0[20]/Geant4 10.04.p01.[15] The physics parameter settings in GATE/Geant4 were chosen under consideration of a publication by Wulff et al.,[9] who investigated the configuration of ionization chamber simulations in proton beams in TOPAS[16]/Geant4.10.03.p1.[15] Wulff et al. showed that with an appropriate physics parameter setting in Geant4, a fano cavity test for protons was passed at a 0.1% level and that f_Q factors determined for two detailed ionization chamber models agreed with those presented by Gomà et al.[6] showing maximum deviations of 0.6% at the highest energy. While Wulff et al. determined f_Q factors for two different physics lists varying in the hadronic interaction models, this work will focus on one of those physics lists by using the binary cascade model (BIC) of Geant4 to simulate the nuclear interactions. Wulff et al. showed that the differences between the two models lead to a maximum deviation of $0.3\% \pm 0.1\%$ at the highest energy.[9] Hence, simulations were performed with physics list QGSP_BIC in combination with EMStandardOpt4 as defined in Geant4.10.04.p1. Within the chamber geometry and a 5 mm margin around it, the production cuts for electrons, positrons, protons, and photons were limited to 1 µm and the maximum step size in this region was set to 1 mm. For electron transport, the Goudsmit-Saunderson MSC model was used together with the fUseSafetyPlus as G4MscStepLimitType. Moreover, the following settings were used for electrons: range factor of 0.2, finalRange of 0.01 mm and dRoverRange of 0.2. Simiele and DeWerd[27] investigated various Geant4 parameters for electron transport and showed that if the Goudsmit–Saunderson MSC model is used with the UseSafetyPlus MSC step limitation in GEANT4 v10.04.p01, which is the case for this work, agreement with theory within 0.5% can be obtained without large step size restrictions. For proton transport a dRoverRange of 0.1, a finalRange of 10 µm and fUseMinimal as the G4MscStepLimitType were used following the study by Wulff *et al.*,[9] who found that an additional reduction of dRoverRange to 0.05, a limitation of the maximum step size to 1 mm and changing the G4MscStepLimitType to fUseDistanceToBoundary for protons did not lead to differences in f_Q outside of the statistical uncertainty for one test simulation for a plane-parallel IBA NACP-02 ionization chamber. A summary of the chosen settings for the simulation in GATE/Geant4 is given in Table III following recommendations by Sechopoulos et al.[26]

The absorbed dose to water $D_{w,Q}$ was calculated in a cylinder with a radius of 1 cm and a thickness of 250 µm.[6–9] All

TABLE III. Simulation settings in GATE/Geant4 used to determine the f_Q factors for various ionization chambers.

Item name	Description	References
Code, version, release date	GATE V8.0 released April 20, 2017 and Geant4 10.04.p01 released on February 28, 2018	Agostinelli et al.,[15] Jan et al.[20]
Validation	Proton transport: Fano cavity test was passed at a 0.1% level; Electron transport: Agreement with theory within 0.5%	Wulff et al.[9]; Simiele and DeWerd[27]
Source description	10×10 cm^2 parallel beam of monoenergetic protons with incident energies of 70, 100, 150, 200, and 250 MeV	
Physics list	QGSP_BIC_EMZ (EMstandardOpt4)	
Electron transport		
MSC model	Goudsmit–Saunderson (E < 100 MeV), WentzelIV (E > 100 MeV)	
MSC range factor	0.2	
MSC step limitation	fUseSafetyPlus	
Skin	3	
e–/e + ionization model	Penelope Ionization (E < 1 MeV), Moller Bhaba (E > 1 MeV)	
dRoverRange	0.2	
Final range	10 μm	
Production cut	1 μm (scoring volume + 5 mm margin), 1 mm (water phantom)	
Maximum step size	1 mm (scoring volume + 5 mm margin)	
Proton transport		
MSC model	WentzelVI M	

ionization chambers were positioned with their reference points at the measurement depth z_Q to simulate the absorbed dose to the ionization chambers' sensitive volumes $D^{\text{Ref}}_{\text{Cham},Q}$. Additionally, to investigate the influence of the displacement effect on the measurement with cylindrical ionization chambers, the absorbed dose $D^{\text{EPOM}}_{\text{Cham},Q}$ was simulated by placing the chambers with their EPOM at the measurement depth. The ratio $\frac{D_{\text{w},Q}}{D^{\text{Ref}}_{\text{Cham},Q}}$ will then give the f^{Ref}_Q factor for the reference point positioning and the ratio $\frac{D_{\text{w},Q}}{D^{\text{EPOM}}_{\text{Cham},Q}}$ defines f^{EPOM}_Q for cylindrical chambers positioned under consideration of their EPOM.

The approaches to determine p_Q factors have been presented in various studies.[8,11,21,22] The simulated absorbed dose values that were determined to calculate the various p_Q for cylindrical chambers are illustrated in Fig. 1. $D_{\text{w},Q}$ was simulated as described above. In a next step, the absorbed dose to the chamber cavity $D_{\text{cav},Q}$ was scored with the central axis, or reference point, of the cavity positioned at the measurement depth z_Q. The ratio $\frac{D_{\text{w},Q}}{D_{\text{cav},Q}}$ inherits two perturbation correction factors, namely p_{cav} and p_{dis}, and the water-to-air stopping power ratio $(s_{\text{w,a}})_Q$. Under consideration of $(s_{\text{w,a}})_Q$ calculated with PENH[13] in Gomà and Sterpin[7] based on the

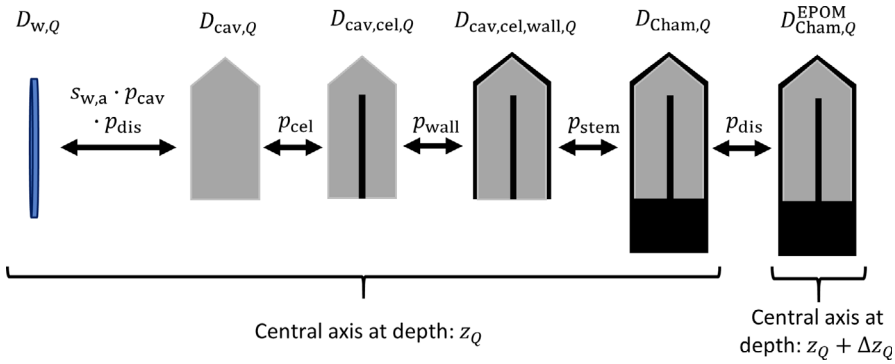

FIG. 1. Illustration of simulated quantities to determine the individual perturbation correction factors for cylindrical ionization chambers. [Color figure can be viewed at wileyonlinelibrary.com]

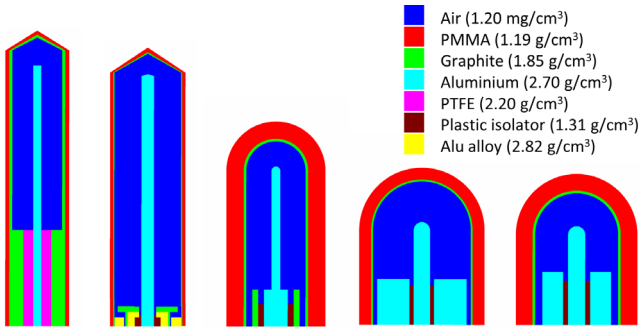

FIG. 2. Geometries (not true to scale) and materials with density given in parenthesis of all cylindrical chambers investigated in this study visualized with egs_view from EGSnrc.[18,19] Geometries from left to right: Farmer chamber NE 2571, PTW Farmer chamber 30013, PTW PinPoint 31014, PTW Semiflex 3D 31021, and PTW PinPoint 3D 31022.

mean excitation energies recommended for water and air in the latest ICRU Report 90 $p_{cav} \cdot p_{dis}$ were separated from the ratio. Because Gomà and Sterpin[7] found an agreement within 0.1% to the $(s_{w,a})_Q$ by Gomà et al.[28] determined in GAMOS/Geant4[14,15] an uncertainty of 0.1% for the $(s_{w,a})_Q$ by Gomà and Sterpin[7] was assumed in this work. The perturbation factors p_{cel}, p_{wall}, and p_{stem} are calculated with simulations, in which the individual chamber parts were added successively, and again by determining the ratio of the corresponding absorbed dose values. Finally, to isolate p_{cav} from p_{dis}, the perturbation correction factor compensating for the displacement effect p_{dis} is determined by calculating the ratio $\frac{D^{Ref}_{Cham,Q}}{D^{EPOM}_{Cham,Q}}$.

For cylindrical ionization chambers, the overall perturbation correction factors p_Q were determined under consideration of the two different positioning approaches. For the reference point positioning, p_Q^{Ref} was determined by the product of all individual factors p_{cel}, p_{wall}, p_{stem}, p_{cav} and p_{dis}. In contrast, when positioning the ionization chamber with its EPOM at the measurement depth, p_{dis} was already corrected for by shifting the chamber by Δz_Q further down in the water phantom during the simulations, such that p_Q^{EPOM} resulted from the product of p_{cel}, p_{wall}, p_{stem} and p_{cav} only. The simulations performed for plane-parallel ionization chambers only consisted of the determination of $D_{cav,Q}$ and $D^{Ref}_{Cham,Q}$ because p_Q for plane-parallel chambers is defined by the product of p_{cav} and p_{wall},[1,22] where the EPOM is considered to lie at the chamber's reference point.

2.D. Investigated ionization chambers

Four plane-parallel and five cylindrical ionization chambers were investigated in this work. Chamber geometries were implemented in the two Monte Carlo codes EGSnrc[18,19] and GATE V8.0/Geant4[15,20] based on construction drawings. The plane-parallel ionization chambers were the NACP-02 (IBA Dosimetry, Schwarzenbruck, Germany), Markus 23343 (PTW Freiburg, Germany), Advanced Markus 34045 (PTW Freiburg, Germany), and Roos 34001 (PTW Freiburg, Germany). As cylindrical chambers, the Farmer chamber NE 2571, Farmer 30013 (PTW Freiburg, Germany), PinPoint 31014 (PTW Freiburg, Germany), Semiflex 3D 31021 (PTW Freiburg, Germany), and PinPoint 3D 31022 (PTW Freiburg, Germany) were studied. Detailed construction drawings of all PTW ionization chambers were provided by the manufacturer. The geometry information for the Farmer chamber NE 2571 was partly taken from Wulff et al.[21] and partly taken from the Phoenix Dosimetry website.[29] The IBA NACP-02 model was based on the one in Wulff et al.[9] The geometries of all cylindrical chambers are illustrated in Fig. 2. Table IV provides information on the plane-parallel chambers. In both Monte Carlo codes, the materials water, air, and graphite were generated by assigning the mean excitation energies $I_{water} = 78$ eV, $I_{air} = 85.7$ eV and $I_{graphite} = 81$ eV following the recommendations of ICRU Report 90.[12] A ratio of $\frac{(W_a)_Q}{(W_a)_{Q_0}} = 1.014 \pm 0.4\%$ is used to calculate k_Q with $(W_a)_Q = 34.44$ eV and $(W_a)_{Q_0} = 33.97$ eV also according to ICRU Report 90.[12]

3. RESULTS

3.A. Monte Carlo simulated f_{Q_0}

The simulated f_{Q_0} factors determined in EGSnrc within this work are presented in Fig. 3 in comparison to f_{Q_0} factors

TABLE IV. Geometry and material description of all plane-parallel chambers investigated in this work.

Ionization chamber	Composition and thickness of entrance window	Electrode spacing [mm]	Collecting electrode thickness	Radius of sensitive volume [mm]	Thickness of guard ring [mm]
IBA NACP-02	0.1 mm mylar (1.39 g/cm^3) 0.5 mm graphite (1.85 g/cm^3)	2	0.05 mm graphite (0.92 g/cm^3) 0.25 mm rexolite (1.05 g/cm^3)	5	3.25
PTW markus	0.87 mm PMMA (1.19 g/cm^3) 0.4 mm air (1.20 mg/cm^3) 0.03 mm PE (0.92 g/cm^3)	2.01	0.03 mm graphite (0.44 g/cm^3)	2.65	0.27
PTW advanced markus	0.87 mm PMMA (1.19 g/cm^3) 0.4 mm air (1.20 mg/cm^3) 0.03 mm PE (0.92 g/cm^3)	1	0.03 mm graphite (0.44 g/cm^3)	2.5	2
PTW roos	1.01 mm PMMA (1.19 g/cm^3) 0.02 mm graphite (0.82 g/cm^3) 0.1 mm PMMA (1.19 g/cm^3)	2.01	0.03 mm graphite (0.44 g/cm^3)	7.8	4

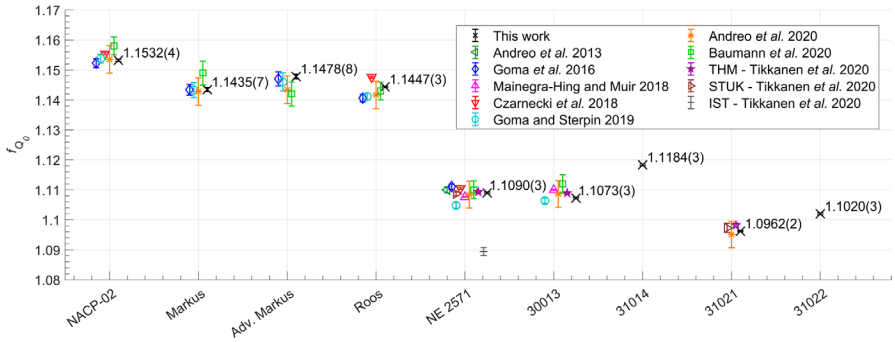

FIG. 3. f_{Q_0} factors simulated with EGSnrc within this work in comparison to values determined based on the ICRU Report 90[12] recommendations presented in literature.[6–8,30,41–44] The f_{Q_0} factors determined in this work are listed next to the corresponding data point. The value within parenthesis corresponds to one standard deviation of the mean with respect to the last digit. [Color figure can be viewed at wileyonlinelibrary.com]

from literature that were simulated under consideration of the latest ICRU Report 90 recommendations.[12]

3.B. Monte Carlo simulated f_Q

Simulated f_Q ratios for all ionization chambers investigated are listed in Table V. For each cylindrical chamber, two values are presented that were determined for the two positioning approaches. Figures 4 and 5 show f_Q for two cylindrical farmer type chambers and those of plane-parallel chambers, respectively, in comparison to literature.

The values of f_Q^{Ref} for cylindrical chambers placed with their reference points at the measurement depth increase with decreasing energy. This increase is most pronounced for large cylindrical chambers like the two Farmer chambers NE 2571 and PTW 30013, where the f_Q^{Ref} between 70 MeV and 250 MeV differ by 4.5%.

The positioning of cylindrical chambers with their EPOM at the measurement depth of 2 cm leads to a reduced energy dependence and nearly constant f_Q^{EPOM} with a maximum variation of 0.6% seen for the PTW Farmer chamber 30013. When comparing the f_Q^{EPOM} and f_Q^{Ref} for individual cylindrical chambers, the difference between both factors decreases with increasing energy. The largest difference between f_Q^{EPOM} and f_Q^{Ref} amounts to 4.5% at 70 MeV for the NE 2571 and still amounts to 0.5% at 250 MeV for both Farmer type chambers.

The f_Q determined for plane-parallel ionization chambers as shown in Fig. 5 are nearly constant over the considered energy range with a maximum difference of 0.8% for the f_Q of the PTW Markus chamber.

3.C. Monte Carlo simulated perturbation correction factors p_Q

Figures 6 and 7 show the simulated perturbation correction factors for the investigated cylindrical and plane-parallel ionization chambers, respectively. The perturbation correction factors for the PTW Roos chamber are compared to a study by Lourenço et al.[11]

Of all the perturbation factors p_{dis} shows the greatest deviation from unity. Figure 6 shows an increase in p_{dis} towards low proton energies for cylindrical ionization chambers. This increase is most pronounced for large cylindrical chambers with an extended air cavity, like the Farmer chambers NE 2571 and PTW 30013, for which the p_{dis} vary from 1.005 ± 0.2% up to 1.045 ± 0.1%. The smallest variation over the energy range of 1.5% is determined for the p_{dis} of the PTW PinPoint 31014. The other individual perturbation correction factors of both chamber types are relatively constant over the considered

TABLE V. Monte Carlo simulated f_Q factors for various ionization chambers and incident proton energies. The value(s) given in parenthesis indicate the standard deviation of the mean with respect to the last digit(s). Note that values for cylindrical chambers are presented for two different positioning approaches.

Chamber and positioning type	Ionization chamber	Energy [MeV]				
		70	100	150	200	250
f_Q plane-parallel, reference point = EPOM	IBA NACP-02	1.1189 (9)	1.1179 (11)	1.1202 (16)	1.1184 (18)	1.1185 (21)
	PTW Markus	1.1368 (11)	1.1336 (14)	1.1294 (18)	1.1337 (19)	1.1275 (25)
	PTW Adv. Markus	1.1362 (14)	1.1318 (14)	1.1294 (15)	1.1307 (19)	1.1326 (20)
	PTW Roos	1.1251 (4)	1.1259 (5)	1.1269 (6)	1.1274 (8)	1.1253 (9)
f_Q^{Ref} cylindrical, reference point	NE 2571	1.1646 (10)	1.1325 (3)	1.1222 (7)	1.1171 (13)	1.1146 (15)
	PTW 30013	1.1670 (5)	1.1348 (5)	1.1228 (8)	1.1216 (8)	1.1172 (10)
	PTW 31014	1.1345 (9)	1.1231 (13)	1.1169 (12)	1.1151 (24)	1.1148 (27)
	PTW 31021	1.1515 (9)	1.1269 (9)	1.1166 (13)	1.1129 (16)	1.1098 (17)
	PTW 31022	1.1368 (13)	1.1207 (17)	1.1120 (12)	1.1127 (16)	1.1079 (29)
f_Q^{EPOM} cylindrical, EPOM	NE 2571	1.1142 (4)	1.1155 (6)	1.1146 (7)	1.1120 (9)	1.1088 (11)
	PTW 30013	1.1184 (5)	1.1175 (6)	1.1144 (8)	1.1140 (9)	1.1115 (9)
	PTW 31014	1.1170 (10)	1.1148 (11)	1.1144 (15)	1.1148 (16)	1.1139 (17)
	PTW 31021	1.1136 (6)	1.1129 (8)	1.1123 (9)	1.1102 (12)	1.1078 (12)
	PTW 31022	1.1134 (9)	1.1120 (11)	1.1107 (14)	1.1108 (18)	1.1096 (19)

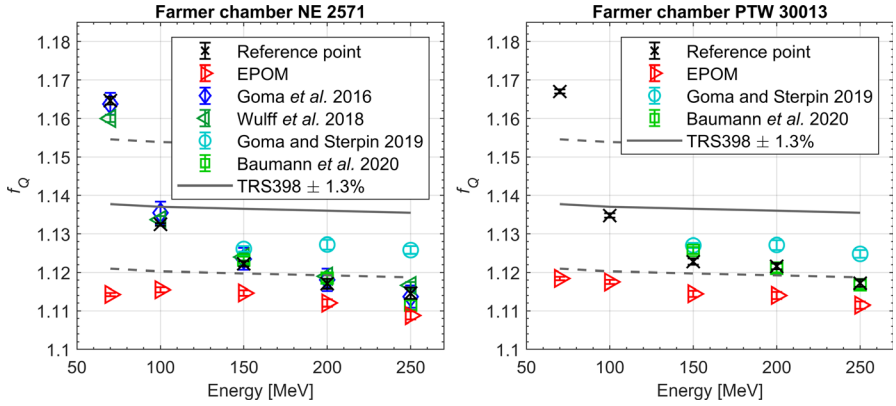

FIG. 4. Monte Carlo simulated f_Q factors for the two positioning approaches (Reference point and EPOM) determined in this work for Farmer type cylindrical ionization chambers in comparison to literature.[1,6–9] [Color figure can be viewed at wileyonlinelibrary.com]

energy range. The most pronounced perturbation among the chamber components is caused by the chamber wall, where the largest correction was found for the PTW PinPoint 3D with $p_{\mathrm{wall}} = 0.981 \pm 0.3\%$ at 250 MeV. The maximum variation within the energy range can be seen for the p_{wall} of the PTW Markus chamber with a maximum difference of 1.5%. The mean value of p_{stem} considering all cylindrical chambers and energies, is 0.996 with a maximum variation of 1.2%. Correspondingly, the mean value of p_{cel} is determined as 0.997 with a maximum variation of 1.3%. The mean perturbation correction factor for the chambers' air cavity p_{cav} was found to be 1.005 with a maximum variation of 0.8% considering both plane-parallel and cylindrical chambers.

For cylindrical ionization chambers, the two different positioning approaches recommended in IAEA TRS-398[1] (reference point) and DIN6801-1[10] (EPOM) resulted in two distinct total perturbation correction factors p_Q^{Ref} and p_Q^{EPOM}. While p_Q^{Ref} increase with decreasing energy with a maximum difference of 4.4% for the Farmer chamber NE 2571, the p_Q^{EPOM} are relatively constant over the considered energy range within 0.7% for the two Farmer chambers, 0.2% for the PTW PinPoint 31014, 0.6% for the PTW Semiflex 3D 31021, and 0.3% for the PTW PinPoint 3D. The total p_Q determined for plane-parallel chambers are also constant in the energy range within 0.3% for the IBA NACP-02 and PTW Roos chamber, 0.7% for the PTW Markus chamber, and 0.5% for the PTW Advanced Markus.

3.D. Beam quality correction factor k_{Q,Q_0}

Figures 8 and 9 show the k_Q for cylindrical and plane-parallel chambers, respectively, in comparison to literature.[1,6–8] The corresponding values are shown in Table VI, where two f_Q factors for cylindrical ionization chambers resulting from the EPOM- and reference point positioning approaches, k_Q^{EPOM} and k_Q^{Ref}, are presented. Because f_{Q_0} for each chamber is constant over the considered energy range, the same observations described above for the f_Q factors also apply for k_Q.

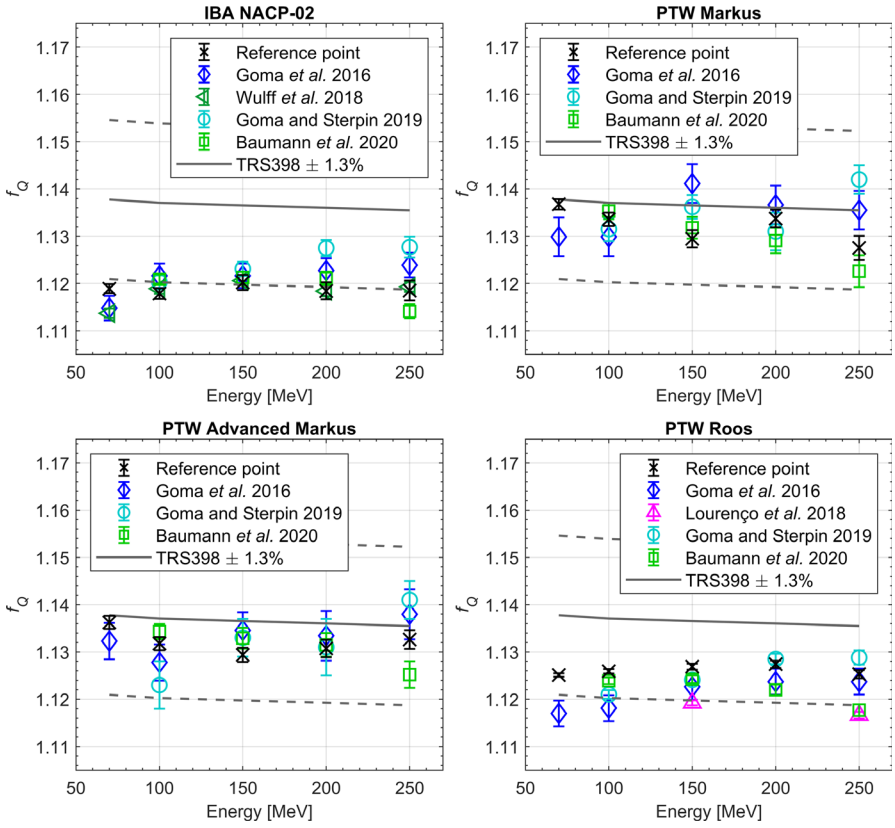

FIG. 5. Monte Carlo simulated f_Q factors of plane-parallel ionization chambers determined in this work (Reference point) in comparison to literature.[1,6,8,9,11] [Color figure can be viewed at wileyonlinelibrary.com]

4. DISCUSSION

4.A. Monte Carlo simulated f_{Q_0}

f_{Q_0} factors determined in this work are in good agreement with the literature (Fig. 3), where the values of f_{Q_0} have been calculated with different Monte Carlo codes considering ICRU Report 90.[12]

Figure 3 shows that the f_{Q_0} factors determined within this work for the plane-parallel chambers agree with those from literature with a maximum difference of 0.5% from the f_{Q_0} for the PTW Advanced Markus chamber calculated by Baumann et al. with TOPAS/Geant4.[8] Considering the f_{Q_0} of the NE 2571, all factors agree within 0.6% when disregarding the outlier from Tikkanen et al.[30] (IST research group), which differs by 1.8% from the result determined in this work. The f_{Q_0} simulated for PTW Farmer chamber 30013 shows a maximum difference of 0.4% to the work by Baumann et al.[8] The f_{Q_0} determined for the PTW Semiflex 3D 31021 chamber in this work agrees within 0.2% with the value presented by Tikkanen et al.[30] (THM research group).

4.B. Monte Carlo simulated p_Q

p_{dis} determined for cylindrical chambers was found to have the greatest contributions to p_Q^{Ref} of up to 1.045 ± 0.1% for large cylindrical ionization chambers at low proton energies. This is a result of the reference point positioning in combination with the dose gradient present at the measurement depth.[4,6,31] It is remarkable that p_{dis} of up to 1.005 is also found at the highest energies for large Farmer chambers. To further examine this finding, the p_{dis} determined for the PTW Farmer chamber 30013 of 1.045 ± 0.1% at 70 MeV and of 1.005 ± 0.1% at 250 MeV was compared to the ratio $\frac{D_w(z_Q)}{D_w(z_Q-\Delta z_Q)}$, which was found to be 1.0439 ± 0.03% at 70 MeV and 1.0049 ± 0.06% at 250 MeV. The good agreement further elucidates the origin of p_{dis} that is directly related to the gradient effect caused by the nonvanishing gradient in the depth dose curve despite the measurement in the plateau region. Therefore, measurement values of a cylindrical ionization chamber placed with its reference point at the measurement depth should be corrected by the displacement correction factors,[32,33] which are dependent on energy. It is noteworthy that p_{dis} is part of the k_Q^{Ref} and f_Q^{Ref} presented in this work such that the application of these factors leads to a correction of the reference point positioning for the depth and energies considered in this study.

The relatively constant p_Q^{EPOM} over the considered energy range indicate that the recommended EPOM of 0.75 times the radius of the sensitive volume of the ionization chambers as provided in DIN6801-1[10] for proton beams is a good estimate for the ionization chambers investigated in this work. This agrees with the observation made by Palmans and Verhaegen[33] and Palmans[34] for most ionization chambers.

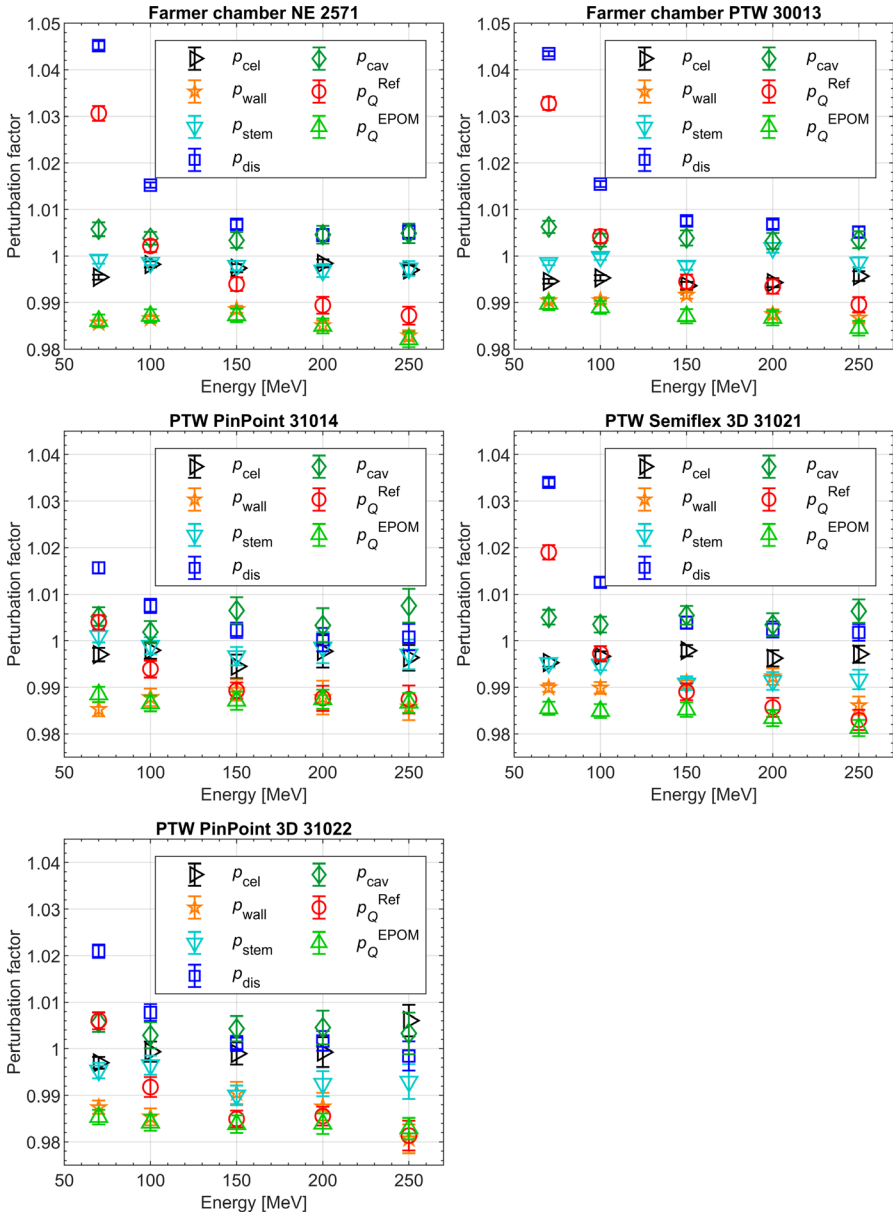

FIG. 6. Monte Carlo simulated perturbation correction factors of cylindrical ionization chambers. Note that the total perturbation correction factors p_Q^{Ref} for the reference point positioning are obtained by the product of p_{cel}, p_{wall}, p_{stem}, p_{dis}, and p_{cav}. In contrast, when positioning the ionization chamber with its EPOM at the measurement depth, p_{dis} is already corrected so that p_Q^{EPOM} results from the product of p_{cel}, p_{wall}, p_{stem}, and p_{cav}. [Color figure can be viewed at wileyonlinelibrary.com]

The p_{cel} presented in this work for the NE 2571, which are on average 0.997, agree with the experimental values determined by Medin et al.[35] and Palmans et al.[32] of 0.997 ± 0.004 in a 170 MeV proton beam and 0.997 ± 0.002 in a 75 MeV proton beam, respectively. Considering secondary electron perturbations only, Palmans[36] presents Monte Carlo calculated p_{wall} and p_{cel} for the NE 2571, which saturate at around 0.985 and 0.998, respectively. Those factors are comparable to the average p_{wall} of 0.986 and p_{cel} of 0.997 determined in this work. Palmans et al.[37] determined ratios of p_Q in a 75 MeV proton beam at a depth corresponding to an R_{res} of 2.65 cm using the Farmer chamber NE 2571 as the reference such that a comparison to p_Q ratios determined in this work for the 70 MeV proton beam ($R_{res} = 2.18$ cm) was possible as shown in Table VII. Because Palmans et al.[37] corrected for gradient perturbations, the $p_Q^{EPOM, NE 2571}$ were used to determine the ratios for this work. A maximum difference of 1.8% was found for the ratio $p_Q^{Markus}/p_Q^{EPOM, NE 2571}$.

Lourenço et al.[11] determined p_Q of the PTW Roos chamber using the Monte Carlo code FLUKA[17] as shown in Fig. 7. While p_{wall} of this work agree with those by Lourenço et al. within 0.3%, the p_{cav} determined by Lourenço et al. is closer to unity with a maximum difference to the p_{cav} determined in this work of 0.6%. Recently, Baumann et al.[8] used the Monte Carlo code TOPASv3.1.p1[16] together with GEANT4.10.03.p1[15] to calculate k_Q factors in monoenergetic proton fields and exemplarily simulated perturbation

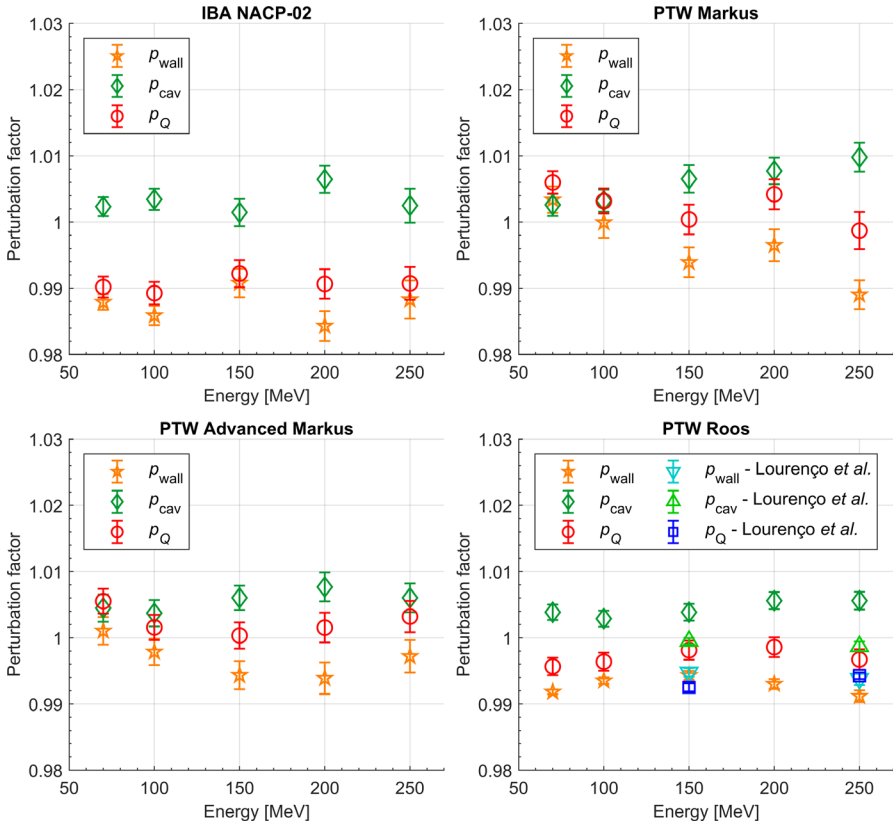

FIG. 7. Monte Carlo simulated perturbation correction factors of plane-parallel ionization chambers. p_Q is obtained by the product of p_{wall} and p_{cel}. The perturbation correction factors determined for the PTW Roos chamber are compared to those determined by Lourenço et al.[11] [Color figure can be viewed at wileyonlinelibrary.com]

correction factors in a 250 MeV proton beam for the individual chamber parts of the cylindrical ionization chamber Exradin A1SL. They found a total p_Q^{Ref} of 0.987(7), where the perturbation from the chamber wall had the largest contribution of 1.5%.[8] This finding is in accordance with this work where the same conclusion for the most pronounced perturbation of all ionization chamber components being the chamber wall can be drawn.

The results in the recent literature and of this work show that the chambers' perturbation correction factors may differ from unity. Consequently, the approximation of $p_Q = 1$ assumed in the dosimetry protocols IAEA TRS-398[1] and DIN6801-1[10] should be revised.

4.C. Monte Carlo simulated f_Q

Considering the two Farmer chambers NE 2571 and PTW 30013, an agreement within 0.4% between the f_Q^{Ref} determined in this work and the f_Q determined by Gomà et al.,[6] Wulff et al.[9] and Baumann et al.[8] is found as depicted in Fig. 4. Although Wulff et al. investigated two different physics lists for simulating the hadronic interactions, for better visibility, Figs. 4 and 5 only include their results for the QGSP_BIC physics list. The influence from the two physics lists was found to be $< 0.3\% \pm 0.1\%$.[9]

The increase in f_Q^{Ref} of the NE 2571 at low proton energies agrees with that described by Gomà et al.[6] and Wulff et al.[9] Baumann et al. only determined f_Q for cylindrical chambers for energies $E \geq 150$ MeV.[8] The increase of f_Q^{Ref} at low energies is a result of the gradient effect as discussed above. Differences of up to 1% are observed when comparing the f_Q^{Ref} of the Farmer chambers to those calculated by Gomà and Sterpin,[7] which are most pronounced at the high proton energies. In contrast to Gomà et al.,[6] this more recent study included the simulation of nuclear interactions and prompt-gamma emission, which was implemented by Sterpin et al.[38]

The f_Q^{EPOM} of cylindrical chambers are nearly constant over the energy range considered. This shows that the positioning of cylindrical chambers with the EPOM at the measurement depth leads to an adequate compensation of the displacement effect. When comparing the f_Q^{EPOM} and f_Q^{Ref} for the chambers in Fig. 4, it can be seen that the factors not only differ at low proton energies, where a comparably steep gradient is present at the measurement depth and a large displacement effect is expected, but also at the highest proton energies where the measurement depth of 2 cm lies in the plateau of the depth dose curve as previously explained for the total perturbation factor p_Q.

The f_Q for plane-parallel chambers in Fig. 5 from the different studies are all relatively constant over the energy range studied. The f_Q determined in this work for the IBA NACP-02 agree with a maximum difference of 0.5% with the data presented by Wulff et al.[9] at 70 MeV. The maximum

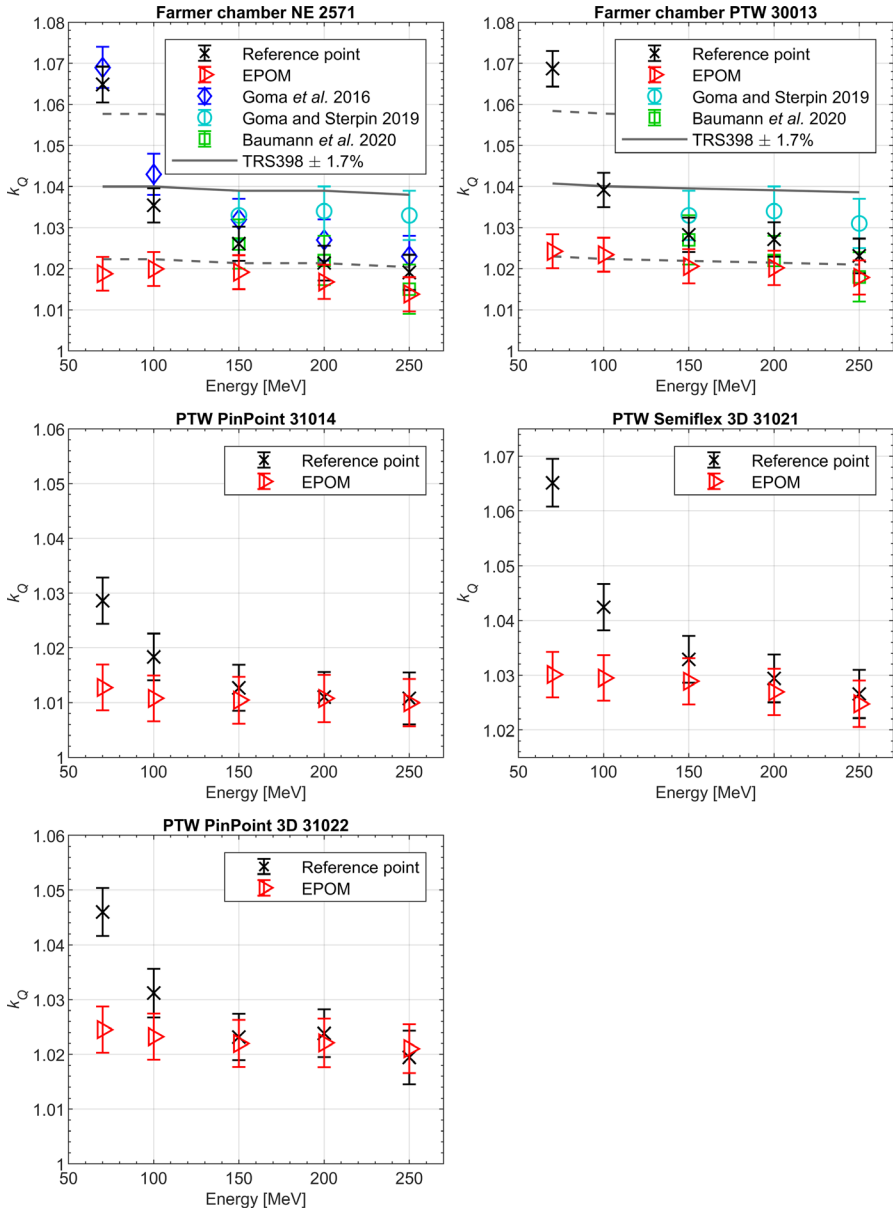

FIG. 8. Monte Carlo simulated k_Q factors for the two positioning approaches (Reference point and EPOM) determined in this work for cylindrical ionization chambers in comparison to literature.[1,6–8] [Color figure can be viewed at wileyonlinelibrary.com]

difference of f_Q for plane-parallel chambers in this work to Baumann et al.[8] is 0.7% for the PTW Roos chamber at 250 MeV. While the f_Q for the PTW Markus and PTW Advanced Markus chamber agree quite well with the f_Q from IAEA TRS-398,[12] the f_Q of the IBA NACP-02 and PTW Roos chamber are up to 1.7% and 1.1% smaller, respectively. Larger deviations are also found at higher energies when compared to the recent publication by Gomà and Sterpin,[7] who claimed nuclear interactions are only considered in the Monte Carlo code PENH used in this more recent study. Baumann et al.[8] further investigated this argument by comparing f_Q simulations in TOPAS/Geant4 where nuclear interactions were either switched off or on and found that the f_Q factors without nuclear interaction simulation were 1.5% higher than those determined with the corresponding physics switched on.[8] Similar conclusions can be drawn from the work by Lourenço et al.[11] who determined p_Q in FLUKA and investigated the impact of nuclear interaction simulation. Lourenço et al. found that p_Q increases when nuclear interactions are disregarded.[11] The findings by Baumann et al. and Lourenço et al. therefore contradict the results by Gomà and Sterpin that indicate that nuclear interaction simulation leads to larger f_Q at high energies.[7,8,11]

4.D. Monte Carlo simulated k_Q

The beam quality correction factors have been determined for four plane-parallel and five cylindrical ionization chambers in this work. A distinction between two positioning approaches has been made resulting in k_Q^{Ref} and k_Q^{EPOM} for

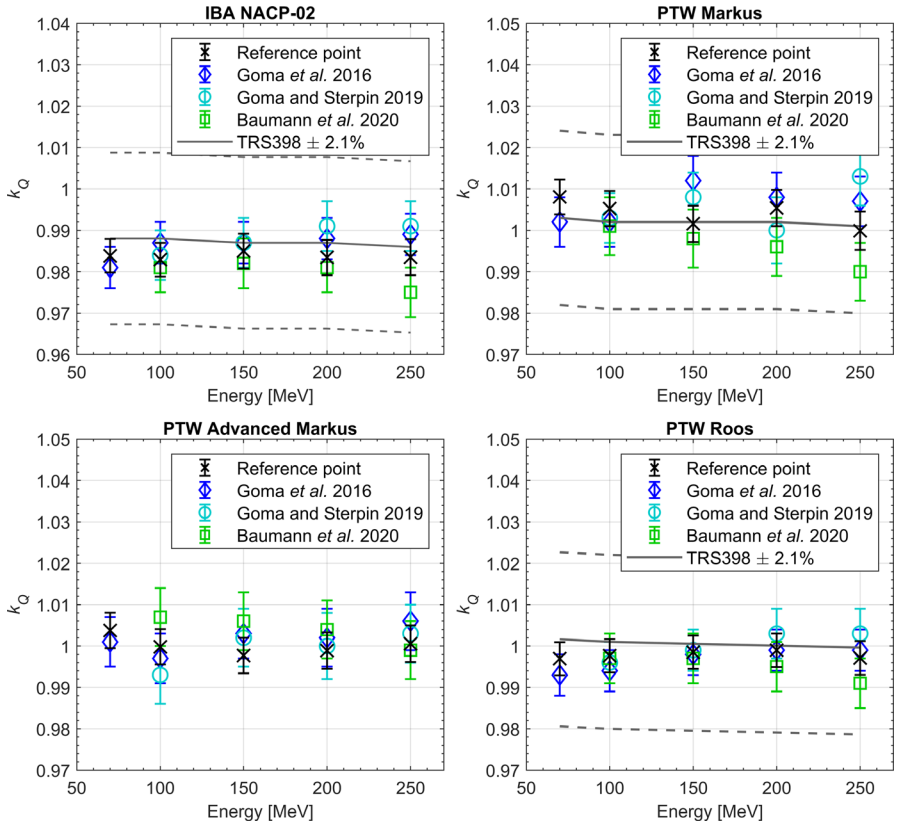

FIG. 9. Monte Carlo simulated k_Q factors of plane-parallel ionization chambers determined in this work (Reference point) in comparison to literature.[1,6–8] [Color figure can be viewed at wileyonlinelibrary.com]

each cylindrical chamber. Despite the scarce data available in the literature for comparisons, where mostly only k_Q^{Ref} has been presented, the values obtained in this work for cylindrical chambers differ from those presented by Gomà et al.[6] and Baumann et al.[8] by a maximum of 0.7%. Gomà and Sterpin[7] and Baumann et al.[8] have only calculated k_Q^{Ref} factors for cylindrical chambers for proton energies $E \geq 150$ MeV, where the impact from the gradient effect is assumed to be less pronounced. Larger differences are found in comparison to the k_Q factors by Gomà and Sterpin[7] with a maximum difference of 1.4% for the Farmer chamber NE 2571 at the highest energy of 250 MeV.

The k_Q^{EPOM} determined in this work for the Farmer chamber NE 2571 can be compared to experimental values obtained by Medin et al.[2] Using water calorimetry as the reference, they determined a k_Q^{EPOM} for the NE 2571 of 1.021 ± 0.7% in a 175 MeV monoenergetic proton beam with $R_{\text{res}} = 14.7$ cm. This value differs from the k_Q^{EPOM} obtained here for the 150 MeV proton field with comparable $R_{\text{res}} = 14.12$ cm by 0.2%. Medin[3] presents a k_Q of 1.032 ± 0.013 for the NE 2571 determined using water calorimetry in a 180 MeV scanned pulsed proton beam with $R_{\text{res}} = 16.5$ cm. No remarks concerning the consideration of the effective measurement depth are made. The k_Q^{Ref} and k_Q^{EPOM} determined in this work at 150 MeV (R_{res} =14.12 cm) for the NE 2571 are both within the uncertainty of the value by Medin[3] with a difference of 0.6% and 1.3%, respectively.

For the plane-parallel chambers IBA NACP-02, PTW Advanced Markus and PTW Roos, a maximum difference of 0.6% was found comparing to the work by Gomà et al.,[6] whereas the maximum difference from the studies by Gomà and Sterpin[7] and Baumann et al.[8] is 0.8% and 0.9%, respectively. The largest differences can be asserted for the PTW Markus chamber, with a maximum difference of 1.3% from the literature.

k_Q/k_Q^{Markus} ratios were determined experimentally by Gomà et al.[4] in a pseudo-monoenergetic field of 174 MeV protons at 15 g/cm^2 depth at $R_{\text{res}} = 5.93$ cm allowing for a comparison to ratios of this work presented in Table VIII. Table VIII reveals a maximum difference to the work by Gomà et al.[4] of 1.7% in the ratio of $k_Q^{30013}/k_Q^{\text{Markus}}$.

In line with previous studies, the data determined in this work show discrepancies of up to 2.6% for k_Q^{Ref} and 2.4% for k_Q^{EPOM} for cylindrical chambers and a maximum difference of 0.6% for plane-parallel chambers from the values recommended in IAEA TRS-398.[1] The large difference between the k_Q^{Ref} and k_Q^{EPOM} for cylindrical chambers shows that reference dosimetry in steep dose gradients should be carried out with caution. Several studies[4,6,31,39] suggested to only perform reference dosimetry with plane-parallel ionization chambers or under consideration of the EPOM if a cylindrical chamber is used. Similar recommendations are provided in the German protocol for proton and light ion dosimetry DIN6801-1[10] by stating that suitable small compact chambers or plane-parallel

TABLE VI. Monte Carlo simulated beam quality correction factors k_Q for various ionization chambers and incident proton energies. The value within parenthesis corresponds to one standard deviation of the mean with respect to the last digit(s). Note that k_Q for the cylindrical chambers are presented for two different positioning approaches.

		Energy [MeV]				
Chamber and positioning type	Ionization chamber	70	100	150	200	250
k_Q plane-parallel, reference point = EPOM	IBA NACP-02	0.9838 (40)	0.9829 (41)	0.9850 (42)	0.9834 (43)	0.9835 (44)
	PTW Markus	1.0081 (42)	1.0052 (43)	1.0016 (44)	1.0054 (44)	0.9999 (46)
	PTW Adv. Markus	1.0038 (43)	0.9998 (43)	0.9977 (43)	0.9989 (44)	1.0006 (44)
	PTW Roos	0.9969 (40)	0.9977 (40)	0.9985 (40)	0.9990 (41)	0.9971 (41)
k_Q^{Ref} cylindrical, reference point	NE 2571	1.0649 (44)	1.0355 (42)	1.0261 (42)	1.0214 (43)	1.0191 (43)
	PTW 30013	1.0687 (43)	1.0392 (42)	1.0282 (42)	1.0271 (42)	1.0231 (42)
	PTW 31014	1.0286 (42)	1.0183 (43)	1.0127 (42)	1.0110 (46)	1.0108 (47)
	PTW 31021	1.0651 (43)	1.0424 (43)	1.0329 (43)	1.0294 (44)	1.0266 (44)
	PTW 31022	1.0460 (44)	1.0312 (44)	1.0232 (43)	1.0238 (44)	1.0194 (49)
k_Q^{EPOM} Cylindrical, EPOM	NE 2571	1.0188 (41)	1.0199 (41)	1.0191 (41)	1.0168 (42)	1.0138 (42)
	PTW 30013	1.0242 (41)	1.0234 (41)	1.0206 (42)	1.0202 (42)	1.0179 (42)
	PTW 31014	1.0127 (42)	1.0108 (42)	1.0104 (43)	1.0108 (43)	1.0100 (43)
	PTW 31021	1.0301 (42)	1.0295 (42)	1.0289 (42)	1.0270 (43)	1.0248 (42)
	PTW 31022	1.0245 (42)	1.0232 (42)	1.0220 (43)	1.0221 (44)	1.0210 (45)

TABLE VII. $p_Q/p_Q^{\mathrm{EPOM,\ NE\ 2571}}$ ratios as determined experimentally by Palmans et al.[37] in comparison to the corresponding ratios determined in this study. The value within parenthesis corresponds to the standard uncertainty in the last digit(s).

	Palmans et al. (R_{res} = 2.65 cm)	This work (R_{res} = 2.18 cm)	Difference [%]
$p_Q^{\mathrm{NACP-02}}/p_Q^{\mathrm{EPOM,\ NE\ 2571}}$	1.006 (6)	1.004 (2)	−0.2
$p_Q^{\mathrm{Markus}}/p_Q^{\mathrm{EPOM,\ NE\ 2571}}$	1.002 (5)	1.020 (2)	1.8
$p_Q^{\mathrm{Roos}}/p_Q^{\mathrm{EPOM,\ NE\ 2571}}$	1.000 (3)	1.010 (2)	1.0

TABLE VIII. $k_Q/k_Q^{\mathrm{Markus}}$ ratios as determined experimentally by Gomà et al.[4] in comparison to the corresponding ratios determined in this study. The value within parenthesis corresponds to the standard uncertainty in the last digit(s).

	Gomà et al. (R_{res} = 5.93 cm)	This work (R_{res} = 5.9 cm)	Difference [%]
$k_Q^{30013}/k_Q^{\mathrm{Markus}}$	1.051 (8)	1.0338 (59)	−1.7
$k_Q^{\mathrm{NACP-02}}/k_Q^{\mathrm{Markus}}$	0.989 (8)	0.9778 (59)	−1.1
$k_Q^{\mathrm{Roos}}/k_Q^{\mathrm{Markus}}$	1.007 (8)	0.9924 (58)	−1.4
$k_Q^{\mathrm{Adv.\ Markus}}/k_Q^{\mathrm{Markus}}$	0.996 (8)	0.9946 (60)	−0.1

chambers should be used for reference dosimetry at residual ranges smaller than 1.5 cm and that the EPOM should be considered. The relatively constant k_Q^{EPOM} for cylindrical and k_Q for plane-parallel chambers indicates that positioning according to the EPOM may allow the use of energy-independent beam quality correction factors, which in these cases appear to be more practicable and less prone to errors. DIN6801-1 proposes such constant k_Q^{EPOM} for monoenergetic proton beams with residual ranges larger than 1.5 cm arguing that the variance is 0.2%, although this work shows that the associated variations can be up to 0.8%. It is also noteworthy that while IAEA TRS-398 suggests considering the EPOM in carbon ion fields, this approach is currently not recommended for proton fields.[1]

The k_Q^{Ref} presented here are listed with a combined type A uncertainty for f_{Q_0} and f_Q determined in this work and the type B uncertainty for the W_{a} ratio. Type B uncertainties for f_Q/f_{Q_0} ratios of at least 0.3% were estimated in Wulff et al.[9] and Baumann et al.,[8] where the same underlying code (Geant4) has been used for the calculations of both factors. In this work, the f_{Q_0} factors have been calculated using the well-benchmarked code EGSnrc for photon beams, which is more efficient, and allows for better comparability to the literature, whereas the factors f_Q were simulated using GATE/Geant4. Therefore, the Type B uncertainty associated with the f_Q/f_{Q_0} ratios presented here may differ from the estimation in Wulff et al.[9] and Baumann et al.[8] due to differences in the cross-section data and particle transport of the codes. Baumann et al.[40] investigated the impact of combining a f_Q factor determined in TOPAS/Geant4 and a f_{Q_0} calculated in EGSnrc and found that the resulting difference from using the same code for both factors is (0.3 ± 0.2)%.

The new mean excitation energies for water, air, and graphite as recommended in the ICRU Report 90 have been considered in both Monte Carlo codes by using user-generated materials instead of the standard material database. Direct comparisons between the stopping powers of the materials used in this work to the tabulated values in ICRU Report 90 have been performed exemplarily for 50 MeV, 100 MeV, 150 MeV, and 200 MeV protons. The electronic stopping powers agree within 0.15% for water and air and within 0.33% for graphite and are consequently well within the uncertainty listed in the ICRU Report 90. It is noteworthy that the ICRU 90 stopping powers for protons have been directly implemented in Geant4 recently.

5. CONCLUSIONS

k_Q and p_Q were determined for five cylindrical and four plane-parallel ionization chambers in monoenergetic proton beams. To the best of our knowledge, k_Q for the three cylindrical ionization chambers, PTW Semiflex 31021, PTW PinPoint 31014, and PTW PinPoint 3D 31022, have not been determined so far for monoenergetic proton fields. For cylindrical ionization chambers, the influence on k_Q from the two commonly used positioning procedures, reference point and EPOM, has been investigated over the energy range from 70 MeV to 250 MeV, within which the respective values have been compared. The difference in k_Q from the two positioning approaches amounts up to 4.5% at 70 MeV and still half a percent at the highest proton energy investigated, 250 MeV, showing that the positioning is critical even at higher energies.

The chamber's perturbation correction factors have been found to differ from unity, underlining the findings from recent publications[6–9,11] and providing more rationale for revising the approximation of p_Q being unity currently made in IAEA TRS-398[1] and DIN6801-1.[10] Among these perturbation factors, the energy-dependent displacement effect correction factors p_{dis} for cylindrical ionization chambers contribute the greatest to p_Q, whereas the chamber wall causes the largest perturbation among the individual chamber components.

ACKNOWLEDGMENTS

The authors thank Jörg Wulff for fruitful discussions, providing the TOPAS/Geant4 input file of the plane-parallel chamber IBA NACP-02 and the f_Q factors determined in their work in private communication. Moreover, we thank Kilian Baumann, Ana Lourenço, and Joonas Tikkannen for providing the numerical values of their results. We thank Sytze Brandenburg and Emiel van der Graaf from the KVI Center for Advanced Radiation Technology Groningen for fruitful discussions on the presented results. The authors would like to thank PTW Freiburg for providing the construction drawings of detectors investigated in this work. Open access funding enabled and organized by Projekt DEAL.

CONFLICT OF INTEREST

The authors have no conflict to disclose.

[a]Author to whom correspondence should be addressed. Electronic mail: jana.kretschmer@uni-oldenburg.de.

REFERENCES

1. Andreo P, Burns DT, Hohlfeld K, et al. Absorbed Dose Determination in External Beam Radiotherapy: An International Code of Practice for Dosimetry Based on Standards of Absorbed Dose to Water. Technical Reports Series No. 398. International Atomic Energy Agency; 2000.
2. Medin J, Ross CK, Klassen NV, Palmans H, Grusell E, Grindborg J-E. Experimental determination of beam quality factors, k_Q, for two types of Farmer chamber in a 10 MV photon and a 175 MeV proton beam. *Phys Med Biol*. 2006;51:1503–1521.
3. Medin J. Implementation of water calorimetry in a 180 MeV scanned pulsed proton beam including an experimental determination of k_Q for a Farmer chamber. *Phys Med Biol*. 2010;55:3287–3298.
4. Gomà C, Hofstetter-Boillat B, Safai S, Vörös S. Experimental validation of beam quality correction factors for proton beams. *Phys Med Biol*. 2015;60:3207–3216.
5. Vatnitsky SM, Siebers JV, Miller DW. k_Q factors for ionization chamber dosimetry in clinical proton beams. *Med Phys*. 1996;23:25–31.
6. Gomà C, Andreo P, Sempau J. Monte Carlo calculation of beam quality correction factors in proton beams using detailed simulation of ionization chambers. *Phys Med Biol*. 2016;61:2389–2406.
7. Gomà C, Sterpin E. Monte Carlo calculation of beam quality correction factors in proton beams using PENH. *Phys Med Biol*. 2019;64:185009.
8. Baumann K-S, Kaupa S, Bach C, Engenhart-Cabillic R, Zink K. Monte Carlo calculation of beam quality correction factors in proton beams using TOPAS/GEANT4. *Phys Med Biol*. 2020;65:055015.
9. Wulff J, Baumann K-S, Verbeek N, Bäumer C, Timmermann B, Zink K. TOPAS/Geant4 configuration for ionization chamber calculations in proton beams. *Phys Med Biol*. 2018;63:115013.
10. DIN 6801–1: 2019–09: Dosismessverfahren Nach Der Sondenmethode Für Protonen- Und Ionenstrahlung - Teil 1: Ionisationskammern; 2019.
11. Lourenço A, Bouchard H, Galer S, Royle G, Palmans H. The influence of nuclear interactions on ionization chamber perturbation factors in proton beams: FLUKA simulations supported by a Fano test. *Med Phys*. 2019;46:885–891.
12. Seltzer SM, Fernández-Varea JM, Andreo P, et al. Key data for ionizing radiation dosimetry: measurement standards and applications. ICRU Report 90. *J ICRU*. 2016;14:1–110.
13. Salvat F. A generic algorithm for Monte Carlo simulation of proton transport. *Nucl Instrum Methods Phys Res Sect B Beam Interact Mater At*. 2013;316:144–159.
14. Arce P, Ignacio Lagares J, Harkness L, et al. Gamos: A framework to do Geant4 simulations in different physics fields with an user-friendly interface. *Nucl Instrum Methods Phys Res Sect Accel Spectrometers Detect Assoc Equip*. 2014;735:304–313.
15. Agostinelli S, Allison J, Amako K, et al. Geant4—a simulation toolkit. *Nucl Instrum Methods Phys Res Sect Accel Spectrom Detect Assoc Equip*. 2003;506:250–303.
16. Perl J, Shin J, Schümann J, Faddegon B, Paganetti H. TOPAS: An innovative proton Monte Carlo platform for research and clinical applications: TOPAS: an innovative proton Monte Carlo platform. *Med Phys*. 2012;39:6818–6837.
17. Ferrari A, Sala PR, Fasso A, Ranft J. FLUKA: A Multi-Particle Transport Code. Report No. SLAC-R-773; 2005. https://doi.org/10.2172/877507.
18. Kawrakow I. Accurate condensed history Monte Carlo simulation of electron transport. I. EGS nrc, the new EGS4 version. *Med Phys*. 2000;27:485–498.
19. Kawrakow I, Mainegra-Hing E, Rogers DWO, Tessier F, Walters BRB. The EGSnrc Code System: Monte Carlo Simulation of Electron and Photon Transport. Technical Report PIRS-701, National Research Council Canada (2017).
20. Jan S, Benoit D, Becheva E, et al. GATE V6: a major enhancement of the GATE simulation platform enabling modelling of CT and radiotherapy. *Phys Med Biol*. 2011;56:881–901.
21. Wulff J, Heverhagen JT, Zink K. Monte-Carlo-based perturbation and beam quality correction factors for thimble ionization chambers in high-energy photon beams. *Phys Med Biol*. 2008;53:2823–2836.
22. Zink K, Wulff J. Beam quality corrections for parallel-plate ion chambers in electron reference dosimetry. *Phys Med Biol*. 2012;57:1831–1854.
23. Wulff J, Zink K, Kawrakow I. Efficiency improvements for ion chamber calculations in high energy photon beams: efficiency improvements for ion chamber calculations. *Med Phys*. 2008;35:1328–1336.
24. Kawrakow I. Accurate condensed history Monte Carlo simulation of electron transport. II. Application to ion chamber response simulations. *Med Phys*. 2000;27:499–513.

25. Mora GM, Maio A, Rogers DWO. Monte Carlo simulation of a typical 60Co therapy source. *Med Phys*. 1999;26:2494–2502.
26. Sechopoulos I, Rogers DWO, Bazalova-Carter M, et al. RECORDS: improved Reporting of montE CarlO RaDiation transport Studies: report of the AAPM Research Committee Task Group 268. *Med Phys*. 2018;45:e1–e5.
27. Simiele E, DeWerd L. On the accuracy and efficiency of condensed history transport in magnetic fields in GEANT4. *Phys Med Biol*. 2018;63:235012.
28. Gomà C, Andreo P, Sempau J. Spencer-Attix water/medium stopping-power ratios for the dosimetry of proton pencil beams. *Phys Med Biol*. 2013;58:2509–2522.
29. Ionisation Chambers – Phoenix Dosimetry. Accessed April 22, 2020. https://phoenix-dosimetry.co.uk/ionisation-chambers/.
30. Tikkanen J, Zink K, Pimpinella M, et al. Calculated beam quality correction factors for ionization chambers in MV photon beams. *Phys Med Biol*. 2020;65:075003.
31. Gomà C, Lorentini S, Meer D, Safai S. Proton beam monitor chamber calibration. *Phys Med Biol*. 2014;59:4961–4971.
32. Palmans H, Verhaegen F, Denis J-M, Vynckier S, Thierens H. Experimental p_{wall} and p_{cel} correction factors for ionization chambers in low-energy clinical proton beams. *Phys Med Biol*. 2001;46:1187–1204.
33. Palmans H, Verhaegen F. On the effective point of measurement of cylindrical ionization chambers for proton beams and other heavy charged particle beams. *Phys Med Biol*. 2000;45:L20–L22.
34. Palmans H. Perturbation factors for cylindrical ionization chambers in proton beams. Part I: corrections for gradients. *Phys Med Biol*. 2006;51:3483–3501.
35. Medin J, Andreo P, Grusell E, Mattsson O, Montelius A, Roos M. Ionization chamber dosimetry of proton beams using cylindrical and plane parallel chambers. N_w versus N_K ion chamber calibrations. *Phys Med Biol*. 1995;40:1161–1176.
36. Palmans H. Secondary Electron Perturbations in Farmer Type Ion Chambers for Clinical Proton Beams. International Atomic Energy Agency (IAEA): IAEA 2011.
37. Palmans H, Verhaegen F, Denis J-M, Vynckier S. Dosimetry using plane-parallel ionization chambers in a 75 MeV clinical proton beam. *Phys Med Biol*. 2002;47:2895–2905.
38. Sterpin E, Sorriaux J, Souris K, Vynckier S, Bouchard H. A Fano cavity test for Monte Carlo proton transport algorithms: fano cavity test for MC simulations of protons. *Med Phys*. 2013;41:011706.
39. Palmans H, Vatnitsky SM. Comment on 'Proton beam monitor chamber calibration'. *Phys Med Biol*. 2016;61:6585–6593.
40. Baumann K-S, Horst F, Zink K, Gomà C. Comparison of penh, fluka, and Geant4/topas for absorbed dose calculations in air cavities representing ionization chambers in high-energy photon and proton beams. *Med Phys*. 2019;46:4639–4653.
41. Andreo P, Wulff J, Burns DT, Palmans H. Consistency in reference radiotherapy dosimetry: resolution of an apparent conundrum when ^{60}Co is the reference quality for charged-particle and photon beams. *Phys Med Biol*. 2013;58:6593–6621.
42. Mainegra-Hing E, Muir BR. On the impact of ICRU report 90 recommendations on k_Q factors for high-energy photon beams. *Med Phys*. 2018;45:3904–3908.
43. Czarnecki D, Poppe B, Zink K. Impact of new ICRU Report 90 recommendations on calculated correction factors for reference dosimetry. *Phys Med Biol*. 2018;63:155015.
44. Andreo P, Burns DT, Kapsch R-P, et al. Determination of consensus k_Q values for megavoltage photon beams for the update of IAEA TRS-398. *Phys Med Biol*. 2020;65:095011.
45. Seco J, Verhaegen F. *Monte Carlo Techniques in Radiation Therapy*. 1st edn. Boca Raton, FL: CRC/Taylor & Francis; 2013. https://doi.org/10.1201/b13961
46. MATLAB. Version 9.7.0.1190202 (R2019b). Natick, Massachusetts: The MathWorks Inc.; 2019.